Chinese Chemical Letters 33 (2022) 2648–2652

Contents lists available at ScienceDirect

Chinese Chemical Letters

journal homepage: www.elsevier.com/locate/cclet

Revisiting the anodic stability of nickel-cobalt hydroxide/carbon composite electrodes for rechargeable Ni-Zn battery

Qihang Liu[a], Xiaoli Zhao[a,*], Xiaowei Yang[a,b,*]

[a] School of Materials Science and Engineering, Interdisciplinary Materials Research Center, Tongji University, Shanghai 201804, China
[b] School of Chemistry and Chemical Engineering, Frontiers Science Center for Transformative Molecules, Shanghai Jiao Tong University, Shanghai 200240, China

ARTICLE INFO

Article history:
Received 12 August 2021
Revised 5 September 2021
Accepted 9 September 2021
Available online 16 September 2021

Keywords:
Rechargeable Ni-Zn battery
Nickel-cobalt hydroxide
Carbon substrates
Anodic stability
Affinity

ABSTRACT

Aqueous rechargeable Ni−Zn batteries are considered as a new generation of safe and reliable electrochemical energy storage system. However, low electronic conductivity of Ni-based cathodes hinders the practical application of Ni-Zn batteries. This problem can be overcome by compositing the Ni-based cathode with highly conductive carbon substrates. A chemical oxidation pre-treatment is popularly applied to the carbon substrates to increase their hydrophilicity and thus facilitate the growth of active materials in aqueous systems. However, the anodic stability of the oxidized carbon substrates is greatly challenged, which has never been addressed in previous reports. In this work, we first compared the anodic stability of carbon fiber paper with and without oxidation treatment and find that carbon substrate with the chemical treatment caused remarkable oxidization current in the required voltage range. To take both anodic stability and fine growth of active materials into account, here we demonstrated a facile physical surface-treatment method of ethanol wetting to replace the chemical treatment. The ethanol infiltration removes gas adsorption on carbon substrates and thus promotes their hydrophilicity. This cost-effective strategy simultaneously achieves a high anodic stability and a fine growth and uniform distribution of nickel-cobalt hydroxide on the carbon microfibers. The resulting Ni-Zn battery provides a high discharge capacity of 219 mAh/g with an operation cell voltage of 1.75 V.

The demand for renewable energy sources in modern society has promoted the development of electrochemical energy storage devices [1–4]. Lithium-ion batteries are the most widely commercialized electrochemical energy storage devices at present, but limited lithium resources and the safety issue have impeded the further applications [5,6]. Zn based aqueous rechargeable batteries have attracted widespread attention due to their distinct advantages including high abundance on Earth, low electrode potential (−1.26 V *versus* standard hydrogen electrode) in alkaline solutions and high safety [7–10]. In particular, Ni-Zn batteries have drawn increasing research interests because of their outstanding merits such as high output voltage (~1.75 V) and eminent theoretical specific energy density (~372 Wh/kg) [11,12].

Layer double hydroxides (LDH) can be represented by a generic formula of $[M^{2+}_{1-x}M^{3+}_{x}(OH)_2][A^{n-}]_{x/n}\cdot zH_2O$, where M^{2+} and M^{3+} represent the divalent and trivalent metallic cation, A^{n-} refers to a non-framework charge compensating anion. LDH are regarded as potential electrode materials in advanced secondary batteries due to their abundant electrochemical active sites and efficient mass transport path provided by unique layered structure [13,14]. Nickel–cobalt layered double hydroxides (NiCo-LDH) have more stable framework than $Ni(OH)_2$ for long-term cycling, as a result of the presence of Co^{3+} ions that mitigates the Jahn–Teller effect of Ni^{3+} ions [15]. The synergistic effect between transition metals ions also makes NiCo-LDH deliver higher capacity and energy density than their individual transition metal counterparts [16,17]. Several researches have been carried out to bring superiority of this LDH into full play. Wang *et al.* grew NiCo-LDH nanosheets on Co-based metal–organic framework to create 3D hierarchical architectures. The resultant NiCo-LDH electrode with more active sites kept 80% retention after 20-fold current increase, which remarkably surpass the performances of nickel hydroxide and cobalt hydroxide [16]. Zhang *et al.* massively synthesized 3D flower-like NiCo-LDH microspheres for supercapacitors. The positive materials could deliver an excellent capacitance about 2228 F/g, which reflected significant potential of for practical application [17]. Though much progress has been made in active material structure optimization

* Corresponding authors at: School of Chemistry and Chemical Engineering, Frontiers Science Center for Transformative Molecules, Shanghai Jiao Tong University, Shanghai 200240, China.
E-mail addresses: zxl36@tongji.edu.cn (X. Zhao), yangxw@sjtu.edu.cn (X. Yang).

https://doi.org/10.1016/j.cclet.2021.09.040
1001-8417/

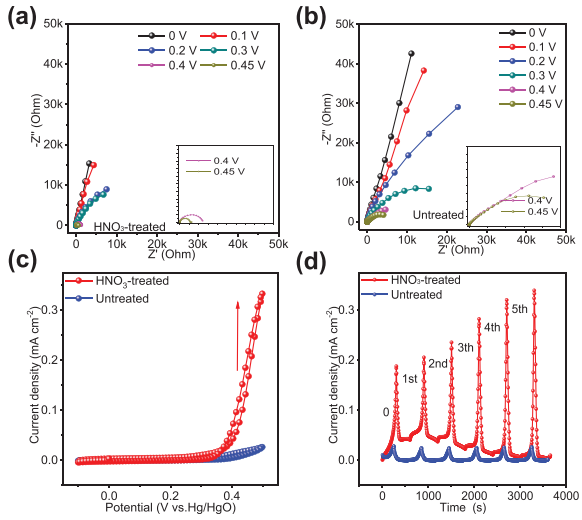

Fig. 1. (a, b) EIS of HNO_3-treated (a) and untreated carbon papers (b) under different potentials. The inset is the magnified high frequency region. (c) CV curves of HNO_3-treated and untreated carbon papers in 6 mol/L KOH at a scan rate of 5 mV/s. (d) Current *vs.* time curves in successive 5 cycles of CV scan.

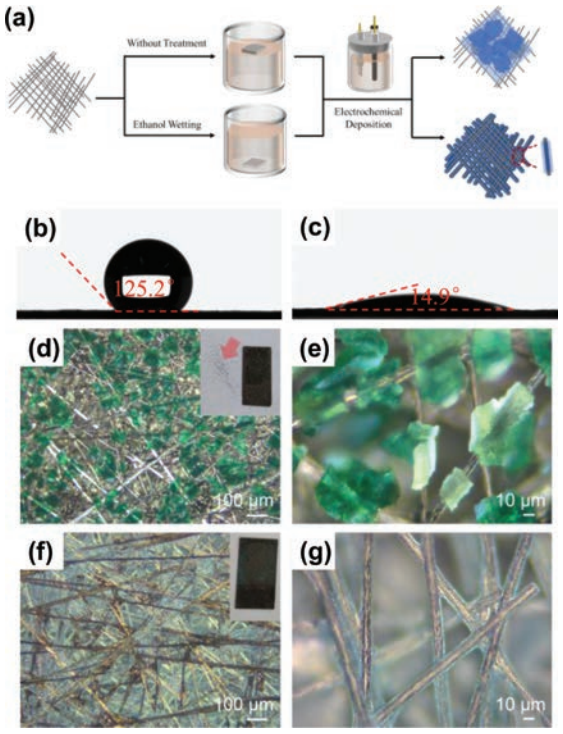

Fig. 2. (a) Schematic of electrochemical deposition of NiCo-LDH on ethanol pre-wetting and untreated carbon paper substrates. Contact angles of water on (b) untreated and (c) ethanol pre-wetting carbon paper substrates. Optical microscopic images of (d, e) C-NiCo-LDH and (f, g) E-NiCo-LDH. The photos in the inset show morphologies of the carbon papers after deposition. The NiCo-LDH particles detach from C-NiCo-LDH, while they stay well on E-NiCo-LDH.

of Ni cathodes, the intrinsic low electronic conductivity limits their high rate performance in the demanding market nowadays [18–20].

One possible solution to this challenge is to composite the active material with a conductive substrate [21–24]. The high density of the metal foam substrate will decrease the total gravimetric energy densities of the devices [25,26]. In such context, the lightweight carbon materials are a more desirable current collectors [27,28]. Carbon papers made up of micron-sized carbon fibers have high electronic conductivity and specific surface area, which facilitates the transport of electrons and ions [29,30]. However, the hydrophobicity of the carbon substrate brings new challenges on active materials growth in aqueous solutions [31]. To enhance the hydrophilicity of carbon substrates, oxidation treatment (*e.g.*, HNO_3) have been adopted to increase the oxygen-containing functional groups on the carbon fibers surface [32]. Nevertheless, when used as the substrates for cathode materials, the anodic stability of carbon is greatly challenged, which has never been addressed in previous reports.

Herein, we present a facile method to electrochemically deposit NiCo-LDH on ethanol pre-wetted carbon paper substrates for a highly anodically stable composite cathode for Ni-Zn battery. The ethanol pre-wetting treatment distinctly increases the NiCo-LDH precursor affinity of carbon paper substrates, benefitting the heterogeneous nucleation. The affinity mediation effect of ethanol treatment is ascribed to a quick removal of adsorbed gas. The obtained NiCo-LDH nanosheets are vertically and uniformly anchored on the microfibers of the carbon paper. Importantly, ethanol pre-wetting treatment does not induce chemical defects into the carbon papers, avoiding impairing its anodic stability even at the potential of 0.5 V *vs.* Hg/HgO, which is important for the capacity exploiting of NiCo-LDH. The assembled NiCo-LDH//Zn battery delivers a large specific capacity of 219 mAh/g at 2 A/g and a good capacity retention within 650 cycles at 5 A/g.

The carbon papers, consisting of carbon microfibers (Fig. S1 in Supporting information), are hydrophobic and cannot keep immersed in water by itself. The effect of HNO_3 treatment on the anodic stability of carbon papers were tested by electrochemical impedance spectroscopy (EIS) under different potentials (*vs.* Hg/HgO) and cyclic voltammetry (CV) scan. As shown in Figs. 1a and b, under increasing potential, the shapes of Nyquist plots gradually change from linear line (ascribed to capacitive behavior) to a semicircle, which indicates the occurrence of charge-transfer reactions. Also, the charge transfer resistance at 0.4 V and 0.45 V of the carbon paper oxidized by HNO_3 is significantly lower than that of the untreated carbon paper, suggesting that the charge transfer reaction for the carbon paper with HNO_3 treatment is easier. Meanwhile, CV of carbon papers shows that there is negligible increase in the current when the potential increases for the carbon papers without HNO_3 treatment, while there is a drastic current increase in the case of HNO_3-treated ones (Fig. 1c). Moreover, in the current *vs.* time curves from 5 cycles of CV scan, the HNO_3-treated carbon papers show increasing maximum anodic currents in cycles, indicating their continuous deterioration (Fig. 1d). As seen, HNO_3 treatment indeed impairs the anode stability of the carbon paper substrates.

Similar to the carbon paper after HNO_3 oxidation, the carbon paper wetted with ethanol sinks into precursor solution easily. In contrast, untreated carbon paper would float on the surface (Fig. 2a). As shown in Figs. 2b and c, the contact angle on the ethanol pre-wetting carbon paper substrates (14.9°) is much smaller than that of the untreated one (125.1°). These results indicate the remarkably improved hydrophilicity of the carbon substrates wetted with ethanol. The untreated carbon paper, HNO_3 treated carbon paper and ethanol pre-wetted carbon paper were used to deposit NiCo-LDH in precursor solutions by pulsed current electrochemical method. The reaction equations of electrochemical deposition are shown below [33]:

$$NO_3^- + 6H_2O + 8e^- \rightleftharpoons NH_3 + 9OH^- \quad (1)$$

$$M^{2+} + 2OH^- \rightleftharpoons M(OH)_2 (M = Co, Ni) \quad (2)$$

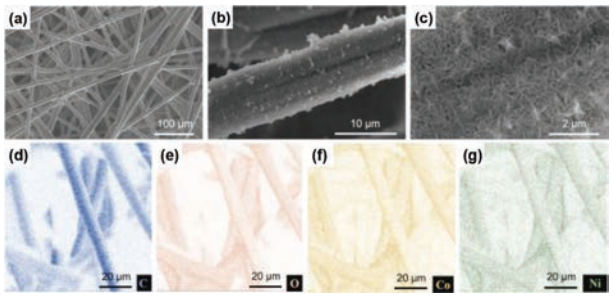

Fig. 3. (a–c) SEM images of E-NiCo-LDH at different magnifications. (d–g) EDX mapping images of C, O, Co and Ni.

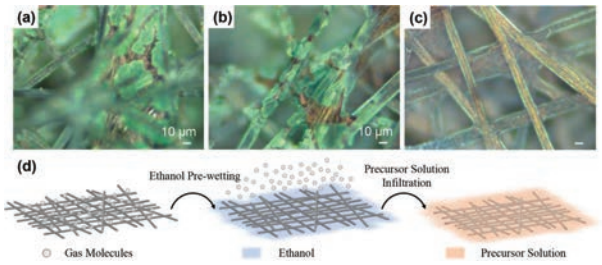

Fig. 4. (a–c) Optical microscopic images of C-NiCo-LDH deposited in the precursor solution with 50 vol% ethanol with deferent pre-immersion time: (a) C-NiCo-LDH_M(0 h), (b) C-NiCo-LDH_M(6 h) and (c) C-NiCo-LDH_M(9 h). (d) Schematic of improving affinity between carbon paper and electrolyte by ethanol wetting to remove gas adsorption.

The obtained products were denoted as C-NiCo-LDH, H-NiCo-LDH and E-NiCo-LDH, respectively. Compared with E-NiCo-LDH, the deposition of NiCo-LDH on C-NiCo-LDH is rather non-uniform and only deposited on the macroscopic surface of carbon paper, meaning that the untreated carbon paper is poorly soaked with the electrolyte and that the electrochemical deposition reaction takes place only on the surface. The NiCo-LDH on untreated carbon papers are tens of micrometers in size observed (Figs. 2d and e), so that the deposited particle would easily be detached from the carbon paper substrates (inset in Fig. 2d). The microscopic morphology was further studied by scanning electron microscopy (SEM) and energy dispersive X-ray spectroscopy (EDS) (Fig. S2 in Supporting information). The NiCo-LDH on C-NiCo-LDHs are so thick that the carbon element signals can be totally covered under EDS mapping. On the contrary, as for H-NiCo-LDH and E-NiCo-LDH, the NiCo-LDH is well dispersed on the 3D carbon papers, and all the carbon fibers are almost completely covered (Fig. 3 and Fig. S3 in Supporting information). Active materials are in the form of nanosheets instead of micrometer-sized particles in C-NiCo-LDH, which can be ascribed to that enhanced wettability increases the number of nucleation sites. The nanosheets grow vertically on the surface of carbon fibers (Fig. 3c) and the resultant porous nanostructure allows an easy access of electrolyte to the entire nanosheets. EDS mapping data (Figs. 3d–g) also confirm a uniform coating of the NiCo-LDH layer. It also ensures that electrons can be transferred directly from the carbon substrate to the active material, thus shortening the electron transport paths, which mitigates the problem of poor intrinsic conductivity of NiCo-LDH. The synthesized E-NiCo-LDH was characterized by X-ray diffraction (XRD) (Fig. S4 in Supporting information). The weak and broad peaks are ascribed to the (003) and (012) crystalline plane of NiCo-LDH, which indicates the deposited NiCo-LDH is amorphous.

How does a simple pre-wetting of ethanol increase the hydrophilicity of carbon papers? In order to gain in-depth understanding of the role of ethanol, a series of control experiments were conducted. Untreated carbon substrates were immersed in a mixture of precursor salt solution and ethanol of different volume fractions. When the untreated substrate is immersed in the precursor solution without ethanol, there is no obvious change on the surface of carbon paper (Fig. S5a in Supporting information). Unlike in neat aqueous solution, a large number of small bubbles appear on the surface of the untreated substrate when it is immersed in the electrolyte containing 50 vol% ethanol. With increasing the ethanol content from 50 vol% to 90 vol%, the bubbles become less (Figs. S5b–d in Supporting information). When the untreated carbon paper immersed in neat ethanol, there is no obvious bubbles (Fig. S5e in Supporting information). When the ethanol pre-wetted carbon paper was immersed in the precursor solution, no bubbles emerge, either (Fig. S5f in Supporting information).

Although the addition of ethanol to the precursor solution can also improve the wettability of the electrolyte to carbon papers (Fig. S6 in Supporting information), we found the immersion time before electrochemical deposition also matters a lot for the depositing morphology of LDH. According to previous study, the volume of ethanol in the precursor solution affects the growth of the active material on the surface of the carbon substrate during the hydrothermal process. When the ethanol content is low, the nanoflakes are not enough to cover the carbon substrate, while when the ethanol content is too high, particles and aggregations would be formed [34]. Therefore, we set the ethanol content to 50 vol% and immersion time before deposition of 0 h, 6 h and 9 h. The obtained samples were denoted as C-NiCo-LDH_M(0 h), C-NiCo-LDH_M(6 h) and C-NiCo-LDH_M(9 h). Figs. 4a–c and Fig. S7 (Supporting information) display their morphologies under optical microscopy. Compared with C-NiCo-LDH (Figs. 2d and e), the NiCo-LDH on C-NiCo-LDH_M(0 h) grows more uniformly on the carbon fibers, but there are still some bulk crystals. The sizes of the bulk crystals decrease as the immersion time in the mixture increases. NiCo-LDH of C-NiCo-LDH_M(9 h) distributes as uniform as on E-NiCo-LDH which is pre-wetted in neat ethanol for only 5 min (Figs. 2f and g). As seen, the ethanol pre-wetting method is much time-efficient than the mixture solvent approach.

These results remind the wetting property of graphene, which has been proved to be intrinsically hydrophilic, though graphene always behaves hydrophobic due an adsorption of hydrocarbon contamination [35]. Accordingly, we propose that the ethanol pre-wetting treatment increases the hydrophilicity of carbon fibers by removing the adsorbed gas molecules (as schematically shown in Fig. 4d) The air cannot be removed when the carbon paper is immersed in the neat precursor solutions, so no bubbles appear (Fig. S5a). The addition of ethanol in the precursor solution drives the air out in the form of bubbles that can be seen by naked eyes. When it is in the case of neat ethanol pre-wetting, we propose that the adsorbed air is removed in the form of very small bubbles that cannot be observed by naked eyes (Figs. S5e and f). Note that all the carbon papers used above were pre-washed by hydrochloric acid, ethanol and deionized water in turn (see Experiment). Therefore, we can exclude the mechanism that neat ethanol washes away the hydrophobic oil adsorbed on the carbon fibers.

As mentioned above, the anodic instability of HNO_3-treated carbon papers is fatal to the electrochemical performance of the composite H-NiCo-LDH, as indicated by the galvanostatic charge-discharge curve of the first cycle. The strong parasitic reactions at high potential leads to a voltage plateau at 0.38 V (*vs.* Hg/HgO), as shown in Fig. S8 (Supporting information). On the contrary, the E-NiCo-LDH can be successfully charged to the set voltage of 0.45 V (*vs.* Hg/HgO) and delivers a satisfying Coulombic efficiency. Since oxygen evolution reaction (OER) starts at nearly 0.6 V (*vs.* Hg/HgO) (Fig. S9 in Supporting information), the tail around 0.38V in galvanostatic charging curve probably originates from carbon oxidization rather than electrolyte decomposition. We can infer that, for

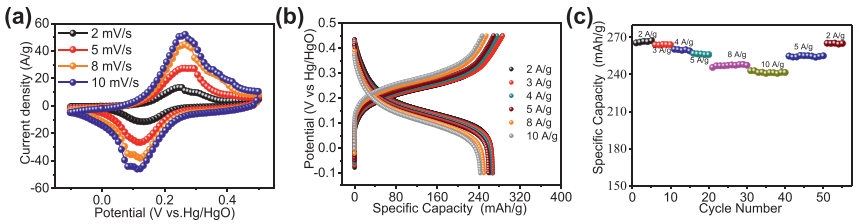

Fig. 5. Electrochemical performance of E-NiCo-LDH. (a) CV curves at different scan rates range from 2 mV/s to 10 mV/s. (b) Galvanostatic charge/discharge profiles at different current densities from 2 A/g to 10 A/g. (c) Rate performance.

H-NiCo-LDH, the carbon is still oxidized before NiCo-LDH is fully charged, even though the carbon microfibers are well covered by NiCo-LDH. We propose that even in the case that the carbon microfibers are totally physically separated from the electrolyte by the covered NiCo-LDH, the carbon with defects would be oxidized by the NiCo-LDH at their charged state. Altogether, the ethanol-pre-wet treatment in this work demonstrates its prominent advantage in terms of the anodic stability, compared with the generally used HNO_3 treatment method.

Furthermore, we investigated the electrochemical performance of E-NiCo-LDH *via* a standard three-electrode setup with 6 mol/L KOH as the electrolyte. The CV curves at scan rates from 2 mV/s to 10 mV/s all show a pair of redox peaks (Fig. 5a). According to the charge storage mechanism of hydroxide [36,37], the redox reaction involved can be written as follows, with M stands for Co or Ni:

$$M(OH)_2 + OH^- \rightleftarrows MOOH + H_2O + e^- \quad (3)$$

The corresponding galvanostatic charge-discharge curves are shown in Fig. 5b, displaying an obvious potential plateau at 0.2 V (*vs.* Hg/HgO). E-NiCo-LDH also shows a good rate performance. The capacity is as high as 260 mAh/g at 2 A/g, and remains around 240 mAh/g as the current density increases to 10 A/g Fig. 5c). Cycling performance was further taken with the galvanostatic charge-discharge measurement at a current density of 5 A/g. As shown in Fig. S10 (Supporting information), the as-obtained E-NiCo-LDH can remain around 200 mAh/g after 500 cycles, demonstrating the stability of the electrode.

To further demonstrate the advantages of E-NiCo-LDH, we also investigated the performance of E-NiCo-LDHs//Zn battery. The operating voltage of the cells reaches 1.9 V. The CV curves show a pair of redox peaks with the scan rate ranging from 2 mV/s to 20 mV/s (Fig. 6a). The galvanostatic discharge plots show a clear output voltage plateau in the region of 1.4 V to 1.6 V, even at a high current density of 10 A/g (Fig. 6b). The capacity reaches 219 mAh/g at a current density of 2 A/g, and 109 mAh/g at a current density of 10 A/g. Moreover, it delivers fairly good cycle stability within 650 charge/discharge cycles at 5 A/g (Fig. 6c). The energy density and capacity of the system were calculated with different charge/discharge depths of the zinc anode (Fig. 6d). The energy density maintains 89.85 Wh/kg even at a charge/discharge depth of 10%. At a charge/discharge depth of 50%, the energy density reaches 215 Wh/kg at a power density of 1.75 kW/kg and remains at 126 Wh/kg even at a power density of up to 11.6 kW/kg.

In this work, we report a facile and effective method to increase the active material precursor-affinity of carbon materials without compromising the anodic stability of the composite electrodes. We prove that the normally used HNO_3 treatment of the carbon substrates would result in an inevitable oxidation of the carbon substrates when operating at high potentials, which induces electronic network deterioration and charging difficulty of the cathodes. The ethanol-pre-wetting treatment facilitates the defect-less carbon papers to act as effective substrates that offer abundant heterogeneous nucleation sites for the deposition of active materials. Based on the control experiments results, we propose that a simple swell

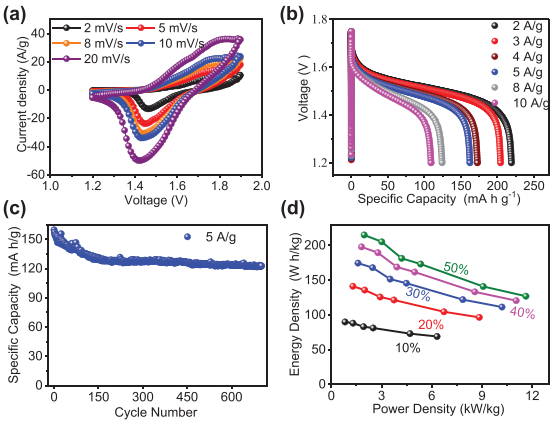

Fig. 6. Electrochemical performance of an E-NiCo-LDH//Zn battery system. (a) CV curves at different scan rates from 2 mV/s to 20 mV/s. (b) Galvanostatic charge/discharge profiles at different current densities from 2 A/g to 10 A/g. (c) Cyclic stability at 5 A/g. (d) Ragone plot under different depths of zinc anode discharge. The capacity and energy density were calculated based on the mass of the active material in the cathode.

of ethanol can remove the air molecules adsorbed on the carbon fibers, thus increasing their compatibility with aqueous precursor solutions. The obtained three-dimensional network of E-NiCo-LDH ensures excellent electron transport and ion accessibility, which makes it have excellent rate performance and high capacity. An assembled full cell consisting of a Zn anode and an E-NiCo-LDH cathode delivers a capacity of 219 mAh/g at a current density of 2 A/g and an output voltage plateau of up to 1.5 V.

Declaration of competing interest

The authors declare that they have no known competing financial interests or personal relationships that could have appeared to influence the work reported in this paper.

Acknowledgments

This work was supported by National Natural Science Foundation of China (No. 21905206), Shanghai Sail Program (No. 19YF1450800).

Supplementary materials

Supplementary material associated with this article can be found, in the online version, at doi:10.1016/j.cclet.2021.09.040.

References

[1] L. Lei, Y. Sun, X. Wang, et al., Front. Mater. 7 (2020) 96.
[2] J.P. Holdren, Science 315 (2007) 737.
[3] C. Liu, X. Yan, F. Hu, et al., Adv. Mater. 30 (2018) 1705713.
[4] S. Li, J. Fu, G. Miao, et al., Adv. Mater. 33 (2021) 2008424.
[5] M. Li, J. Lu, Z. Chen, et al., Adv. Mater. 30 (2018) 1800561.

[6] F.H. Wu, J. Maier, Y. Yu, Chem. Soc. Rev. 49 (2020) 1569–1614.
[7] T. Hosaka, K. Kubota, A.S. Hameed, et al., Chem. Rev. 120 (2020) 6358–6466.
[8] N. Yabuuchi, K. Kubota, M. Dahbi, et al., Chem. Rev. 114 (2014) 11636–11682.
[9] M. Huang, M. Li, C. Niu, et al., Adv. Funct. Mater. 29 (2019) 1807847.
[10] W. Shang, W. Yu, Y. Liu, et al., Energy Storage Mater. 31 (2020) 44–57.
[11] S. Lai, M.L. Jamesh, X. Wu, et al., Rare Met. 36 (2017) 381–396.
[12] Y. Shi, Y. Chen, L. Shi, et al., Small 16 (2020) 2000730.
[13] S. Wang, X. Duan, T. Gao, et al., J. Electrochem. Soc. 167 (2020) 160550.
[14] S. Wang, S.B. Lai, P.S. Li, et al., J. Power Sources 436 (2019) 226867.
[15] J.H. Lee, H.J. Lee, S.Y. Lim, et al., Adv. Funct. Mater. 27 (2017) 1605225.
[16] H. Chen, Z. Shen, Z. Pan, et al., Adv. Sci. 6 (2019) 1802002.
[17] T. Li, G. Li, L. Li, et al., ACS Appl. Mater. Interfaces 8 (2016) 2562–2572.
[18] L. Meng, D. Lin, J. Wang, et al., ACS Appl. Mater. Interfaces 11 (2019) 14854–14861.
[19] W. Shi, J. Mao, X. Xu, et al., J. Mater. Chem. A 7 (2019) 15654–15661.
[10] J. Li, M.K. Aslam, C.G. Chen, J. Electrochem. Soc. 165 (2018) A910–A917.
[21] W. Luo, J. Hayden, S.H. Jang, et al., Adv. Energy Mater. 8 (2018) 1702615.
[22] S. Moeller, S. Barwe, J. Masa, et al., Angew. Chem. Int. Ed. 59 (2020) 1585–1589.
[23] M. Bichat, E. Raymundo-Pinero, F. Beguin, Carbon 48 (2010) 4351–4361.
[24] W. Liu, L. Yu, R. Yin, et al., Small 16 (2020) 1906775.
[25] Z. Pan, Y. Jiang, P. Yang, et al., ACS Nano 12 (2018) 2968–2979.
[26] L. Chen, J. Zeng, M. Guo, et al., J. Colloid Interface Sci. 583 (2021) 594–604.
[27] S. Wang, X. Zhao, X. Yan, et al., Angew. Chem. Int. Ed. 58 (2019) 205–210.
[28] Z. Xiao, S. Wang, X. Yan, et al., Batter. Supercaps 2 (2019) 766–773.
[29] L. Zhang, D. Shi, T. Liu, et al., Mater. Today 25 (2019) 35–65.
[30] M. Govindasamy, S. Shanthi, E. Elaiyappillai, et al., Electrochim. Acta 293 (2019) 328–337.
[31] L. Shen, J. Wang, G. Xu, et al., Adv. Energy Mater. 5 (2015) 1400977.
[32] D.R. Dreyer, S. Park, C.W. Bielawski, et al., Chem. Soc. Rev. 39 (2010) 228–240.
[33] S.B. Kulkarni, A.D. Jagadale, V.S. Kumbhar, et al., Int. J. Hydrog. Energy 38 (2013) 4046–4053.
[34] L. Zhang, H. Gong, Sci. Rep. 5 (2015) 18108.
[35] Z. Li, Y. Wang, A. Kozbial, et al., Nat. Mater. 12 (2013) 925–931.
[36] M. Wehrens-Dijksma, P.H.L. Notten, Electrochim. Acta 51 (2006) 3609–3621.
[37] H. Gao, S. Xin, J.B. Goodenough, Chem 3 (2017) 26–28.